

Effect of vacuum annealings on the electronic properties of clean Si(111) surfaces

S. Bensalah, J.-P. Lacharme, and C. A. Sébenne

Laboratoire de Physique des Solides, Université Pierre et Marie Curie, 75252 Paris CEDEX 05, France

(Received 13 November 1990; revised manuscript received 11 March 1991)

Clean cleaved Si(111) samples of various degrees of doping have been vacuum annealed at increasing temperatures, up to 1150°C and studied *in situ* by photoemission-yield spectroscopy, with low-energy electron-diffraction and Auger-electron-spectroscopy controls. The photoyield-spectrum changes upon annealing of 7×7 reconstructed surfaces are interpreted as a sharp increase of the density of acceptor levels in the surface layer probed by photoemission. The effect starts above 700°C and saturates beyond 1050°C at $(2\pm 1)\times 10^{19}$ acceptor states cm^{-3} ; contamination decreases this *p*-type overdoping effect. It is attributed to the formation of the appropriate number of Si vacancies, which relaxes, and therefore measures, the residual surface stress of the perfect 7×7 reconstruction.

INTRODUCTION

In addition to cleavage under vacuum, the preparation of a clean surface of silicon requires some vacuum annealing. Its role is either to desorb the impurities which have been left by the preliminary preparation, the nature of which is crucial, or to reorder the surface layer after ion bombardment, or both. There are many reasons for the hopefully clean surfaces which come out of various optimized procedures to have some common features and some differences in their morphologies and electronic properties. The details of the final annealing contribute to increasing the similarities or the differences between different surfaces. The present work deals with the changes in bulk electronic properties within less than 50 Å from the surface induced by vacuum annealing of clean cleaved silicon (111) surfaces at increasing temperatures.

It had been noticed long ago that lightly-doped Si(111) wafers cleaned under ultrahigh vacuum by annealing above 1100°C showed a *p*-type doping larger than 10^{15} cm^{-3} extending over several μm from the surface.¹ The same kind of effect had been studied in more detail a few years ago^{2,3} and boron impurities have been found to be responsible for it, through very small surface contamination and diffusion. There, the boron concentration could reach at most 10^{17} cm^{-3} over a few thousand angstroms, that is, altogether, 10^{12} boron atoms per cm^2 . At a smaller scale and sometimes much higher doping levels, redistribution of dopants close to the (111) and (100) surfaces of vacuum-annealed silicon crystals have been observed.^{3,4} The case of boron surface enrichment by vacuum annealing of heavily doped samples (over 10^{19} cm^{-3}) has been well studied recently.⁵⁻¹⁰ The case of lightly doped *n*- or *p*-type samples which, upon annealing, exhibit a high overdoping (this time over 10^{19} cm^{-3} within a very thin layer below the surface) remains to be elucidated. It can be probed only through surface-sensitive techniques. It was studied on Si cleaned wafers¹¹ and was related to a carbon enrichment within the surface layer.

In the present paper a systematic study of the anneal-

ing effect is presented for lightly-doped samples, $n = 4\times 10^{14}$ cm^{-3} , where the initial surface is prepared by cleavage in order to avoid extrinsic impurities and disordering associated with a cleaning procedure. The surface probe which allows us to control the bulk doping in a layer less than 50 Å thick below the surface is the high-resolution photoemission yield spectroscopy. As was shown long ago in the case of clean cleaved silicon, the shape of the yield curve is very sensitive to the doping level of the sample when it reaches 10^{18} cm^{-3} and above.^{12,13} It is related to a simple band-bending effect which is most effective in the present case of very low photon energy photoemission, where the electron escape depth is in the 10–15-Å range.

The paper is organized as follows. After giving some details about the experiments, the yield curves which are expected for various *p*-type doping levels are computed and checked against the measured ones for a few heavily doped *p*-type samples annealed at low temperature (500°C), i.e., without *p*-type overdoping. Then, the results for lightly doped samples, annealed at higher temperatures, are presented and discussed. In particular, the yield curves are compared to computed curves in order to estimate the level of the *p*-type overdoping.

EXPERIMENT

The experiments were performed in a multipurpose ultrahigh-vacuum system which has been described earlier¹⁴ and which accommodated clean surface preparation techniques and surface analysis techniques such as low-energy electron diffraction (LEED), Auger spectroscopy (AES), and electron-energy-loss spectroscopy, together with photoemission yield spectroscopy (PYS). The latter is a measure of the total photoemitted current as a function of photon energy in the threshold region, from about 4.00 to 6.70 eV, with high sensitivity and accuracy.¹²

The samples were silicon single crystal bars about 5×7 mm^2 in cross section, with the long axis along the [111] direction. A notch about 2 mm deep was cut along the

5-mm side, the 7-mm side being the [211] direction. It gave by cleavage under ultrahigh vacuum a clean 2×1 reconstructed (111) surface, about $5 \times 5 \text{ mm}^2$. It was converted into a 7×7 reconstructed surface, with negligible contamination, by annealing at 500°C in a cylindrical open-ended furnace. This homemade furnace had only refractory metals (W and Ta) as hot parts. Its insulating parts were made of vacuum-treated alumina; they stayed at relatively low temperature and were not in view of the sample during annealing cycles. The same furnace was also used, of course, for high-temperature annealing. It was first thoroughly outgassed in the 1250°C range before any new cleave. Then, before any sample annealing, the calibrated furnace was first heated to the desired temperature. Once the pressure was back to normal, around $(1-2) \times 10^{-10}$ Torr, the sample was entered into one end of the furnace and kept there from 3 min up to 1 h, depending on the experiment. Then the sample cooled down at its own rate, after turning off the furnace power supply. It took some time since PYS measurements became possible (dark counting back to normal with about 1 count per 10 sec) only 20 min later.

The temperature calibration was made previously using a special silicon sample drilled down to about 1 mm from the surface entering the furnace, into which a thermocouple was fixed. A second thermocouple inside the furnace was also used and the power supply was current stabilized. The effect of sample depth into the furnace was checked since after each cleave the silicon bar is shorter and possibly different annealing temperatures must be controlled.

In all the experiments, possible contamination was checked using AES and the permanence of the 7×7 reconstruction was controlled by LEED.

EFFECT OF *p*-TYPE DOPING OF SILICON ON PHOTOEMISSION YIELD SPECTRA

Band-bending effects in photoemission from semiconductors have been very well known since the early ages of modern photoemission, and high dopings have been used very early¹² to bring to the same order of magnitude the escape depth λ of electrons through a clean semiconductor surface and the thickness L of the space-charge layer. For *p*-type silicon, the effective Debye length L_D is at room temperature:

$$L_D = (\epsilon\epsilon_0 kT / e^2 N_A)^{1/2} = 4.1 \times 10^3 N_A^{-1/2} \text{ m},$$

and the corresponding electric field close to the surface F_S in the space-charge region is, in the case of a depletion region,

$$\begin{aligned} F_S &= \frac{kT}{eL_D} [2(|v_s| - 1)]^{1/2} \\ &= 8.62 \times 10^{-6} [N_A (|v_s| - 1)]^{1/2} \text{ V/m}. \end{aligned}$$

If we take a barrier height of 0.50 eV, v_s is 20 and for a doping N_A of 10^{24} m^{-3} , F_S is equal to $37.6 \times 10^6 \text{ V/m}$, that is, 3.8 mV/\AA and varies as $N_A^{1/2}$.

In the present photoemission measurements, the photon energy range is very low, 4–6.7 eV, and the escape

depth λ_e is relatively large: by numerical fitting of a set of photoyield spectra taken from variously doped cleaved samples,¹² λ_e has been found to be about 12–15 Å. Most of the valence electrons contributing to the photoemission yield are therefore coming from a layer less than 40 Å thick. A band-bending effect can be observed in the spectra (see Fig. 1) only if the voltage change ΔV over less than 40 Å is larger than the energy resolution of the system, that is, slightly more than kT , or about 30 meV. The surface electric field must then be higher than 0.75 mV/\AA : it is clearly the case when N_A is above 10^{23} m^{-3} (that is, above 10^{17} cm^{-3}), of course, if a surface barrier in the 0.5-eV range does exist.

Another point has to be raised if a quantitative evaluation of the band-bending effect on photoemission yield in heavily doped samples is to be made; that is, the effect of degeneracy which appears in the high 10^{18} cm^{-3} for *p*-type silicon. The situation is illustrated by case (c) of Fig. 1: (a) the valence-band edge is no longer a well-defined limit since the acceptor state band merges into the valence band, (ii) the bulk density of states has an exponential tail which goes deep into the gap, (iii) the Fermi level crosses the pseudo-valence-band-edge at some distance from the surface, giving a nonconducting medium close to the surface and a semimetal in the bulk. The theoretical calculation of the bulk density of states of a heavily doped semiconductor is not a simple problem.¹⁵ In fact, to our knowledge, there are no such results in the case of heavily doped *p*-type silicon, with its light and heavy holes. Anyway, if they existed, they would not be directly applicable to our problem, because, in the surface space-charge region, there is a strong and changing electric field which should significantly modify the density of states.¹⁶

Therefore, our procedure has been the following. Photoemission yield spectra have been recorded for a few differently doped *p*-type silicon samples having undergone low-temperature annealing to induce the 7×7 reconstruction but without any risk of surface over-dop-

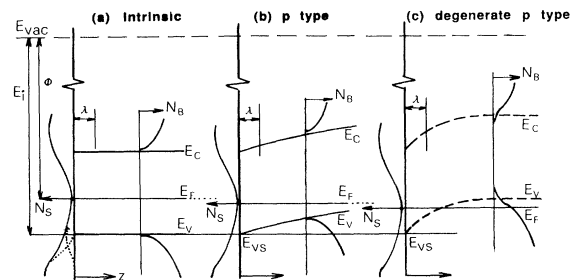


FIG. 1. Schematic of the space-charge region of a silicon (111) surface, (a) for an intrinsic or lightly doped sample, (b) for a moderately doped *p*-type ($\sim 10^{18} \text{ cm}^{-3}$) sample, (c) for a degenerate *p*-type sample ($p \sim 10^{19} \text{ cm}^{-3}$). E_i is the ionization energy, Φ the work function, E_F the Fermi level, E_c and E_v the conduction- and valence-band edges, respectively. Superimposed are the surface density of states $N_S(E)$ and the bulk density of states $N_B(E, z)$. λ is the escape depth of photoemitted electrons.

ing. The results are shown in Fig. 2 on a semilogarithmic plot in order to see more clearly the differences in the threshold region. As expected from case (c) of Fig. 1, the semimetallic behavior of the sample with the highest doping is obvious: at threshold, the photoyield increases exponentially over two or three orders of magnitude with the kT slope of a Maxwellian distribution.

Then these curves have been phenomenologically reproduced in the following way. As drawn in Fig. 1, we have assumed that the ionization energy E_i (5.3 eV for clean Si) and the density of surface states $N_S(E)$ were independent of the doping. We have accepted the experimental evidence of a slight increase of the work function ϕ at high p -type doping levels: the positive surface charge must increase by emptying surface states at Fermi level when the doping increases, in order to keep the equilibrium between the surface and bulk charges. Therefore, the surface barrier decreases slightly. Now, in order to evaluate the bulk state contribution to the yield, we followed the same approach as in Ref. 12, using this time an effective density of bulk states which is at first unknown, $N_B(E, z, N_A)$. The first step has been to parametrize N_B in the most convenient way with respect to the theory¹⁵ and to simplify the calculation. It has

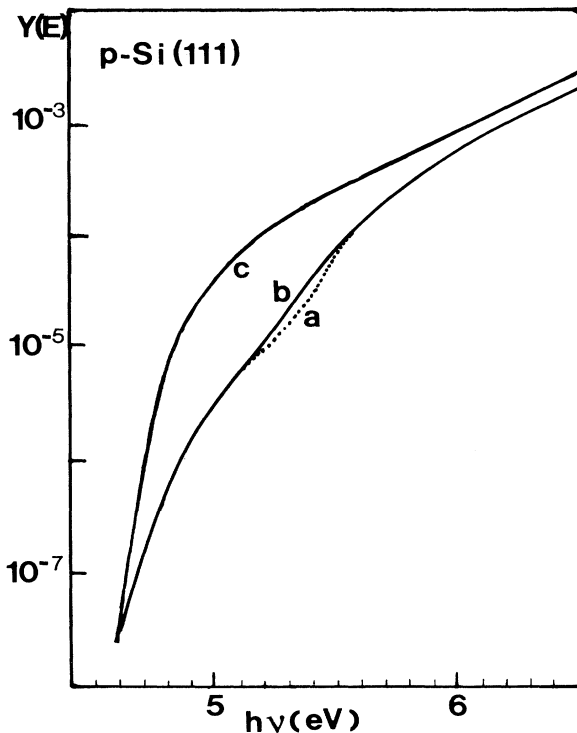


FIG. 2. Semilogarithmic plot of measured photoemission yield spectra, in electron per incident photon, as a function of photon energy for clean silicon (111) 7×7 reconstructed surfaces obtained by cleavage and annealing at 500°C under ultrahigh vacuum (2×10^{-8} Pa). Samples doped at (a) 4×10^{14} P atoms cm^{-3} (lightly doped reference); (b) 1.4×10^{18} B atoms cm^{-3} ; (c) 4×10^{19} B atoms cm^{-3} .

been dissociated into a doping-independent part $N_{B0}(E, z)$, and a doping-dependent impurity band $N_{Bi}(E, z, N_A)$ as illustrated in Fig. 3:

$$N_B(E, z, N_A) = N_{B0}(E, z) + N_{Bi}(E, z, N_A).$$

It has been assumed that the two densities of states do not overlap, but that they are tangent at a pseudo-valence-band-edge E_{vB} . N_{B0} is taken to be of the form $k(E - E_{vB})^{5/2}$ as was found for the lightly-doped samples.¹⁷ N_{Bi} is represented by a rectangular function parametrized by its width ΔE , its height H being determined by the density of acceptors N_A : $H \Delta E = N_A$. The z dependence of both N_{B0} and N_{Bi} arises from the band bending through the change in energy position of E_{vB} across the space-charge region.

The variation $E_{vB}(z)$ is related to the potential distribution $V(z)$ in the space-charge region. The latter is determined by integrating Poisson's equation in which the density of charges $\rho(z)$ at depth z comes from the filled part of the impurity band only. If $f(E)$ is the Fermi Dirac distribution function, we have

$$\rho(z) = N_{Bi}(E, z, N_A) f(E - E_F).$$

Both the exponential tail in the gap and the hole concentration in N_{B0} have been neglected. Given the surface barrier height V_s , the surface electric field $F_s = -(dV/dz)$ at $z=0$, and the position of E_{vB} with respect to E_F far away from the surface, Poisson's equation can be easily integrated numerically for various values of ΔE .

Then the bulk contribution to photoemission is the sum of the contributions of the two densities of filled states, integrated both in energy and in depth, using the voltage distribution found above. Comparison with the measured yield spectra obtained for differently doped samples gives the best values for the ΔE parameter, λ be-

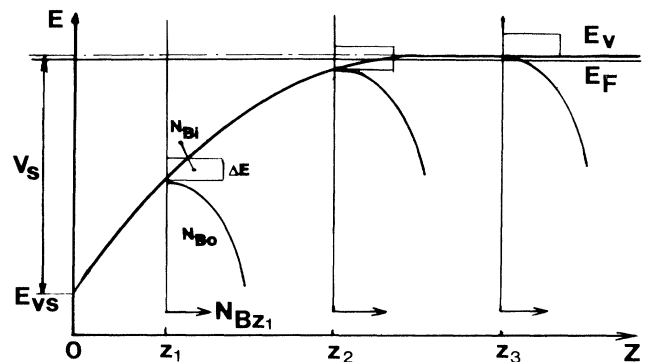


FIG. 3. Model of bulk density of states used to calculate the voltage distribution in the surface space-charge region of heavily doped p -type samples. It is drawn at three depths from the surface to illustrate the occupation changes of these states as a function of distance. E_F is the Fermi level. See text for the other notations.

ing fixed at 12 Å. The density of filled surface states, which has been deduced from the yield spectra of lightly doped samples,^{14,17} is taken care of, at each $h\nu$, either by subtraction from the measured yield curve or by addition to the calculated bulk contribution of its integral from E_F to $h\nu$ below the vacuum level.

Examples of calculated spectra (solid lines) are displayed in Fig. 4 and compared to measured yield curves (dotted curves) for extreme cases of heavily doped p -type samples with $N_A = 1.4 \times 10^{18} \text{ cm}^{-3}$ (case 1) and $N_A = 4 \times 10^{19} \text{ cm}^{-3}$ (case 2). Two values for ΔE come out of these comparisons: either 0.025 eV for $N_A < 10^{19} \text{ cm}^{-3}$ or 0.05 eV otherwise. The fits are satisfactory considering the crude approximations which have been made. They show that the model reproduces the quantitative behavior of the yield spectra as the level of p -type doping changes, and that it can be used, as in the next part, to evaluate the doping of unknown p -type surface layers.

PHOTOEMISSION YIELD SPECTRA OF VACUUM ANNEALED Si(111)

After cleavage in ultrahigh vacuum, the clean Si(111) surface is characterized by a well-known 2×1 reconstruc-

tion and specific electronic properties thoroughly studied by various methods including PYS. Upon vacuum annealing, the surface irreversibly transforms into a new reconstruction at a temperature which depends on the sample but which is never lower than about 200°C. This new clean surface may show a (7×7) LEED diagram or only a (1×1) pattern with background, but all the ingredients which make up the ordered structure are there, that is, adatoms, dimers, stacking faults, and vacancies, and the main features of the new surface electronic structure are always observable. Let us recall that the surface density of filled states is essentially made of three peaks located at the valence-band edge E_{vs} , 0.6 eV, and 1.5 eV below E_{vs} , respectively.¹⁸ The first two are schematically shown in Fig. 1(a) and are well observable in PYS.¹⁷

Typical changes of the photoemission yield spectra upon vacuum annealing of a lightly doped Si(111) sample are shown in Fig. 5. Curve 1 corresponds to the cleaved unannealed 2×1 surface, given as a proof of the good quality of the cleave. Curve 2 is typical of a moderately annealed sample at a temperature where the $2 \times 1 \rightarrow 7 \times 7$ transformation occurs: such curves are obtained up to a maximum temperature of 750°C for 3 min, or lower for longer annealing times. Surfaces with a higher density of defects are not as well structured around E_{vs} and show a

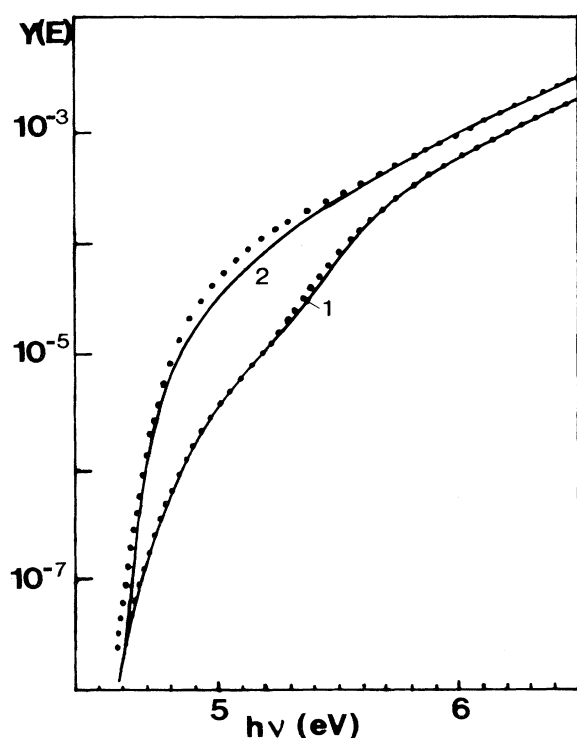


FIG. 4. Semilogarithmic plot of the computed photoemission yield spectra (solid lines) of clean Si(111) 7×7 surfaces using the density of states modeled in Fig. 3 with (1) $N_A = 1.4 \times 10^{18} \text{ cm}^{-3}$ and $\Delta E = 0.025 \text{ eV}$; (2) $N_A = 4 \times 10^{19} \text{ cm}^{-3}$ and $\Delta E = 0.05 \text{ eV}$. The dotted curves come from Fig. 2 with the appropriate densities of acceptors.

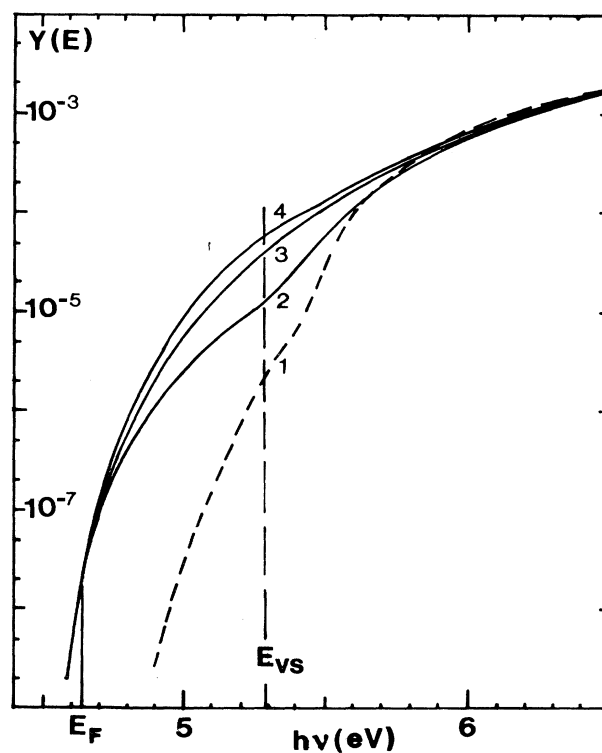


FIG. 5. Semilogarithmic plot of the photoemission yield spectra, in electron per incident photon, as a function of photon energy for a clean Si(111) 7×7 crystal n -type doped at $4 \times 10^{14} \text{ P atoms cm}^{-3}$, (1) initially cleaved in ultrahigh vacuum, then annealed for 3 min at (2) $(740 \pm 15)^\circ\text{C}$; (3) $(800 \pm 15)^\circ\text{C}$; (4) $(960 \pm 15)^\circ\text{C}$.

deformed spectrum at lower temperatures. Curves 3 and 4 show the deformation of the yield spectra at temperatures above 750°C, namely, 800°C and 960°C, respectively.

Since the low-energy threshold remains constant after annealings, the work function does not change very much (careful analysis shows an increase by 50 meV at high annealing temperatures, ϕ being 4.60 ± 0.05 eV).

Since the three curves converge nicely in the high photon energy range, neither escape probability changes nor ionization energy changes can be involved. Only two possibilities remain to explain the deformation from curve 1 to curve 3: either a change in the density of surface states or a change in the density of bulk states, at least in how they contribute to photoemission.

At low annealing temperature, as in curve 2, the tail of filled states in the gap, from E_F to E_{vs} , comes only from surface states. If the deformation at high annealing temperature were due to surface states, their density in the gap would have to be multiplied by a factor of about 5 (see integrated effect of gap surface states at $h\nu = E_{vs}$). Since neither LEED nor AES bring any indication that the surface has changed, such an increase of the amplitude of the intrinsic surface-state band located at E_{vs} is not likely. On the contrary, when comparing the effect of annealing in Fig. 5 to that of high *p*-type doping as shown in Fig. 2, the curves look strongly similar. Therefore, we attribute the deformation of the yield curves upon annealing, as shown in Fig. 5, to an effect of thermally induced *p*-type doping in the surface region within at least the depth probed by photoemission yield spectroscopy, that is, at least about 50 Å.

Now comparing measured spectra such as curves 3 and 4 of Fig. 5 to spectra calculated as explained in the preceding section, the thermally induced *p*-type over doping can be quantitatively evaluated. We find here $(1.2 \pm 0.2) \times 10^{19} \text{ cm}^{-3}$ for curve 3 and $(2.2 \pm 0.2) \times 10^{19} \text{ cm}^{-3}$ for curve 4. An example of fit, which assumes a uniform doping throughout the depth probed, is displayed in Fig. 6 to show its accuracy.

Many cleaves have been studied on various lightly doped samples. The main results are as follows.

As far as we can tell, because measurements are made when the sample is back to room temperature, the appearance of the *p*-type over doping is relatively sudden, that is, a difference of 20° between two successive annealings can make the doping pass from the low level (that is, for these measurements, well below 10^{18} cm^{-3}) to $1 \times 10^{19} \text{ cm}^{-3}$.

The over doping saturates always in a relatively narrow range, from 2 to $3 \times 10^{19} \text{ cm}^{-3}$. Annealings up to 1200°C for 7 min have been applied without significant changes.

The presence of impurities such as C, with a high enough concentration to be detected by AES, seems to decrease the saturation value of the *p*-type over doping around $1 \times 10^{19} \text{ cm}^{-3}$.

Poor-quality cleaves, as identified by the lack of sharpness of the density of surface states of the cleaved surface, have the same effect.

On the average, the work function increases by 50 ± 25 meV from low to high doping.

What is the origin of the *p*-type over doping? There are not many defects able to bring a high density of acceptors in a silicon crystal: three substitutional impurities can be considered which are boron, with a large solubility margin,¹⁹ Al, and Ga, with a bulk solubility limit barely sufficient. Another defect must be considered too, usually extremely unstable in the bulk, which is the single vacancy.²⁰

Let us consider first the cases of Al and Ga. These impurities cannot come from the bulk of the samples: their density in the sample is lower than 10^{13} cm^{-3} ; in order to form a layer at least 50 Å thick, doped at $2 \times 10^{19} \text{ cm}^{-3}$, it would be necessary to empty the bulk over 1 cm, which is unthinkable at 800°C, even if the surface were a Al or Ga sink. Then Al or Ga would have come from outside. This cannot be during annealings: it would be in contradiction with the thermal threshold. If contamination were continuous, surface accumulation would be observed with time without annealing, which is not the case. Therefore the *p*-type over doping cannot be due to Al or Ga.

Considering now the case of boron, the same arguments hold. First, a bulk out diffusion leading to a surface accumulation cannot be accepted when the boron concentration is lower than 10^{14} cm^{-3} and the temperature 800°C, because a diffusion time of a few minutes would not be sufficient. Second, if it were a vacuum con-

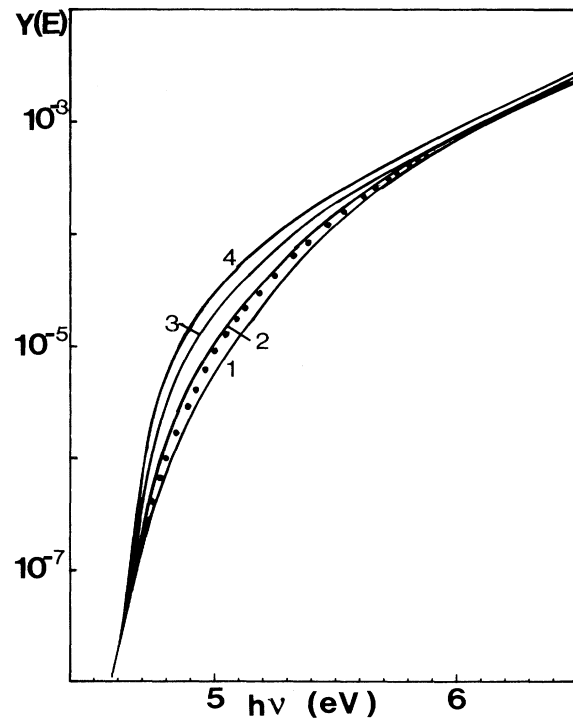


FIG. 6. Semilogarithmic plot of the calculated photoemission yield spectra. Curves 1, 2, 3, and 4 are for *p*-type doping at 1, 2, 3, and $4 \times 10^{19} \text{ cm}^{-3}$, respectively. The dots reproduce the experimental curve at 4 of Fig. 5.

tamination, since the solubility of B in Si is high, the overdoping should not show a definite saturation at most at $3 \times 10^{19} \text{ cm}^{-3}$. Moreover, with time some boron should be detected on the surface by Auger electron spectroscopy, which is not the case. Some B has been seen only when the sample was heavily boron doped from the start and only after annealings in the 1000-°C range.⁵⁻⁹ Otherwise boron contamination is much smaller.³

We are left with the single vacancy as possible *p*-type overdoping defect. The idea is interesting because it would mean that the effect is intrinsic to the Si(111) surface with no impurity involved. However, one has to explain why a very high vacancy concentration would be stable in this surface layer, in contradiction to what is well known in the bulk.²¹ It can be understood if we accept that the 7×7 reconstruction of Si(111) does not achieve the total relaxation of the surface stress. In fact, if a small residual compressive stress is left, the formation of some vacancies below the surface is an elegant way to achieve the relaxation. The 7×7 reconstructed surface has many different local atomic arrangements which keep strains²² and stresses.²³ Our present work would then show that a concentration of 3×10^{19} single bulk vacancies per cm^3 over about 50 Å, that is, 1.5×10^{13} vacancies per cm^2 , completes the relaxation. Compared to the 7.8×10^{14} atoms per cm^2 of the ideal Si(111) surface, it gives roughly one vacancy per 7×7 unit cell randomly distributed close to the surface, which looks quite satisfactory.

Of course, the relaxation can also be achieved by the surface accumulation of substitutional impurities, the radius of which is smaller than that of silicon: it is the reason why boron, carbon, or nitrogen are very difficult to remove from the surface. The relaxation can also be achieved by deposition of a suitable layer which would lead to a less deformed silicon surface: it has been shown

recently in the case of Ga (Ref. 23) and may be generalized to many adsorbed species. Adsorbed layers should also remove the vacancy-induced *p*-type overdoping studied here: it is in agreement with our observation that a slightly carbon contaminated surface needs less vacancies to relax the residual stress.

SUMMARY

The surface space-charge region of a degenerate *p*-type silicon crystal has been modeled and corresponding photoemission yield spectra have been calculated and compared to experiment.

Then it has been shown that vacuum annealing of clean Si(111) 7×7 reconstructed surfaces, at temperatures above as low a limit as 780 °C, induces a *p*-type overdoping along a surface layer no less than 50 Å thick. The acceptor concentration has been quantitatively evaluated and shown to saturate at $3 \times 10^{19} \text{ cm}^{-3}$. The effect must not be taken as a metal-like density of surface states close to the Fermi level since the actual surface-state structures remain unaffected by such treatments. The *p*-type overdoping is attributed to the formation of the adapted concentration of single vacancies, evaluated at 1 per 7×7 surface unit cell, achieving the relaxation of the residual surface stress along the perfect 7×7 reconstruction Si(111) surface.

ACKNOWLEDGMENTS

The authors gratefully acknowledge fruitful discussions with Dr. F. Proix who significantly improved the manuscript. The Laboratoire de Physique des Solides is Unité Associée au Centre National de la Recherche Scientifique No. 154.

-
- ¹J. D. Mottram, A. Thanailakis, and D. C. Northrop, *J. Phys. D* **8**, 1316 (1975).
- ²M. Liehr, M. Renier, R. A. Wachnik, J. Werner, G. S. Scilla, and P. S. Ho, *J. Vac. Sci. Technol. A* **5**, 2131 (1987).
- ³M. Liehr, M. Renier, R. A. Wachnik, and G. S. Scilla, *J. Appl. Phys.* **61**, 4619 (1987).
- ⁴A. Förster, J. M. Layet, and H. Lüth, *Appl. Surf. Sci.* **41**, 306 (1989).
- ⁵S. Bensalah, J.-P. Lacharme, and C. A. Sébenne, *Surf. Sci.* **211/212**, 586 (1989).
- ⁶F. Thibaudau, Ph. Dumas, Ph. Mathiez, A. Humbert, D. Satti, and F. Salvan, *Surf. Sci.* **211/212**, 148 (1989).
- ⁷R. I. Headrick, I. K. Robinson, E. Vlieg, and L. C. Feldman, *Phys. Rev. Lett.* **63**, 1253 (1989).
- ⁸P. Bedrossian, R. D. Meade, K. Mortensen, D. M. Chen, J. A. Golovchenko, and D. Vanderbilt, *Phys. Rev. Lett.* **63**, 1257 (1989).
- ⁹I. W. Lyo, E. Kaxiras, and Ph. Avouris, *Phys. Rev. Lett.* **63**, 1261 (1989).
- ¹⁰E. Kaxiras, K. C. Pandey, F. J. Himpsel, and R. M. Tromp, *Phys. Rev. B* **41**, 1262 (1990).
- ¹¹H. Froitzheim, U. Köhler, and H. Lammering, *Phys. Rev. B* **30**, 5771 (1984).
- ¹²C. Sébenne, D. Bolmont, G. Guichar, and M. Balkanski, *Phys. Rev. B* **12**, 3280 (1975).
- ¹³G. Guichar, C. Sébenne, G. Garry, and M. Balkanski, *Le Vide, Les Couches Minces A* **30**, 97 (1975).
- ¹⁴D. Bolmont, P. Chen, C. A. Sébenne, and F. Proix, *Phys. Rev. B* **24**, 4552 (1981).
- ¹⁵J. Serre and A. Gazhali, *Phys. Rev. B* **28**, 4704 (1983).
- ¹⁶A. Gazhali (private communication); A. Gold, J. Serre, and A. Gazhali, *Phys. Rev. B* **37**, 4589 (1988).
- ¹⁷D. Bolmont, P. Chen, and C. A. Sébenne, *J. Phys. C* **14**, 3313 (1981).
- ¹⁸G. V. Hansson and R. G. Uhrberg, *Surf. Sci. Rep.* **9**, 197 (1988), and references cited therein.
- ¹⁹D. Nobili, *Properties of Silicon* (INSPEC, London, 1988), p. 384.
- ²⁰D. De Cogan, *Properties of Silicon* (INSPEC, London, 1988), pp. 386 and 391.
- ²¹A. R. Peaker and S. Guimaries, *Properties of Silicon* (INSPEC, London, 1988), p. 225.
- ²²I. K. Robinson, W. K. Waskiewicz, P. H. Fuoss, and L. J. Norton, *Phys. Rev. B* **37**, 4325 (1988).
- ²³R. E. Martinez, W. M. Augustyniak, and J. A. Golovchenko, *Phys. Rev. Lett.* **64**, 1035 (1990).